

Investigation of Station Service Transformer Ferroresonance in Manitoba Hydro's 230-kV Dorsey Converter Station

Dr. D. A. N. Jacobson
Manitoba Hydro
820 Taylor Ave.
Winnipeg, Manitoba, R3C 2P4, Canada
dajacobson@hydro.mb.ca

Dr. R. W. Menzies
Dept. of Electrical and Comp. Eng.
University of Manitoba
Winnipeg, Manitoba, R3T 5V6, Canada
menzies@ee.umanitoba.ca

Abstract - An investigation of ferroresonance in a 230-kV transformer is undertaken. Correct modelling of the iron-core losses and the direct magnetic coupling between phases are shown to be important in duplicating field observations. A brute-force time-domain method and an analytical method for displaying margins to ferroresonance on a parameter plane are compared. Following proposed bus modifications, it is shown that loading resistors may now be made switchable.

Keywords: EMTP, field testing, ferroresonance, three-phase transformer, bifurcation, harmonic balance, iron-core loss.

I. INTRODUCTION

The Dorsey 230-kV Converter station is located just north of Winnipeg in the southern portion of the province of Manitoba. It was identified in planning studies several years ago, that twenty-five breakers and current transformers should be replaced and five breakers upgraded in the Dorsey station. The reasons included: wear and tear on existing breakers and spare parts availability but mainly the existing 30-kA short circuit interrupting duty of these breakers is not sufficient following proposed system upgrades. The new breakers are required to have a 63.5-kA interrupting rating at -55° Celsius. As well, the breakers should be able to clear short line faults at up to 90% of the short circuit current rating.

As a result of these specifications, the circuit breaker manufacturer proposed installing multi-head breakers with two breaks/phase and 1500 pF of grading capacitance across each break. In addition, the low temperature high current interrupting rating required a mixing of carbon tetrafluoride (CF_4) with the normal sulphur hexafluoride (SF_6) gas. Following all proposed replacements and upgrades, the maximum total grading capacitance of all parallel breakers has increased from 2000 pF to 7500 pF, following an outage of the longest bus (i.e. 500 m long).

On August 4, 1995, one of the jumbo buses tripped by station service transformer protection due to the catastrophic failure of a 4-kV breaker. The tripping of the 230-kV bus resulted in a ferroresonant condition being established between the station service transformer and the grading capacitance across eleven open 230-kV circuit breakers.

Permanently connected 200- Ω loading resistors were installed on the 4.16-kV secondary bus of two station service transformers in order to mitigate the ferroresonance condition.

A plan is in place to enhance the reliability of the Dorsey

Converter station by adding a third bus and several new bus tie breakers and disconnects. Because of the bus configuration change, there may be an opportunity for removing the loading resistors if the potential for ferroresonance is eliminated.

The paper details an EMTP investigation undertaken to duplicate field recordings taken during the August 4, 1995 ferroresonance event. Correct modelling of the iron-core losses, the magnetization characteristic and the direct magnetic coupling between phases are shown to be extremely important.

Two-dimensional bifurcation diagrams are created using the detailed EMTP model in order to determine margins to ferroresonance on a parameter plane. A single phase analytical model is also created, which can be used to quickly calculate locations of boundaries between different types of ferroresonance oscillation modes. Comparisons are made between the detailed EMTP model and the simplified single-phase analytical model.

II. DESCRIPTION OF AUGUST 5, 1995 DISTURBANCE

On August 5, 1995, at 14:18, Dorsey 4.16-kV breaker 111L failed to latch while attempting to energize a 1500 kW induction motor associated with synchronous condenser SC23. Indications are that the upstream breaker on the low side of station service transformer (SST1) attempted to open to clear the fault but failed. As a result, eleven 230-kV breakers opened to clear bus B2 to which SST1 was connected.

Based on observations of captured oscillographs, one can conclude that the 4.16-kV fault was cleared and the load dropped (i.e. see Fig. 1).

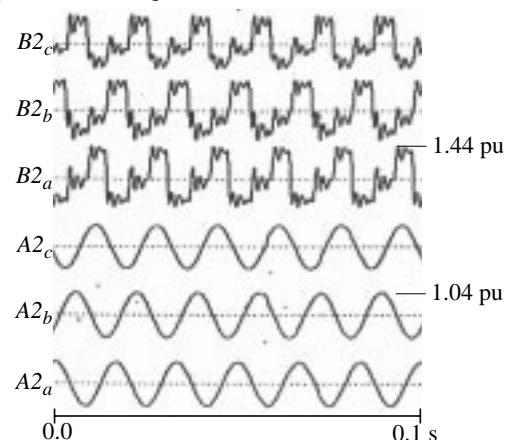


Fig. 1. Field recordings of bus voltages.

Noise levels coming from SST1 were noticeably higher than normal and higher than the nearby loaded SST2 immediately following the 230-kV bus de-energization. Recordings given in Fig. 1 show a very distorted wave shape and overvoltages near 1.5 pu.

The Dorsey synchronous condenser joint var controller responded to the ferroresonant overvoltage on the B2 bus and reduced the var output from the on-line synchronous condensers to near zero. The Dorsey 230-kV voltage on the in-service A2 bus stabilized at approximately 0.91 per unit after 30 minutes. Filter bank F9 was manually switched onto bus B2 at 14:58, eliminating the ferroresonant condition, after other attempts at regaining control of the Dorsey voltage had failed.

III. EMTP MODEL VERIFICATION

An EMTP model of the Dorsey bus was developed and successfully modified to match field recordings of the May 20, 1995 field recordings of the first Dorsey ferroresonant incident [1]. However, this model was unsuccessful in duplicating recordings taken of the August 5, 1995 disturbance.

The problem has been determined to be in the representation of the station service transformer. The original study assumed three single-phase transformers could adequately reproduce the expected transients. The single-phase representation assumes the positive and zero sequence impedances are the same and that there is no coupling between phases. Data was not available to permit accurate modelling of the actual three-phase three-legged core at the time of the original study. Based on studies of another three-phase transformer, accurate transformer modelling has been found to be important [2].

The station service transformer is a 10-MVA, 230-kV grounded-wye/4.16-kV wye transformer. The secondary is grounded through a 2.4 ohm neutral resistor rated at 2400 volts and 1000 amps for 10 seconds. The positive sequence impedance is 12.2%. Since zero sequence short circuit data is not available, a typical value of 89% of the positive sequence is used in an EMTP BCTRAN model. A single-line diagram of the EMTP model is given in Fig. 2.

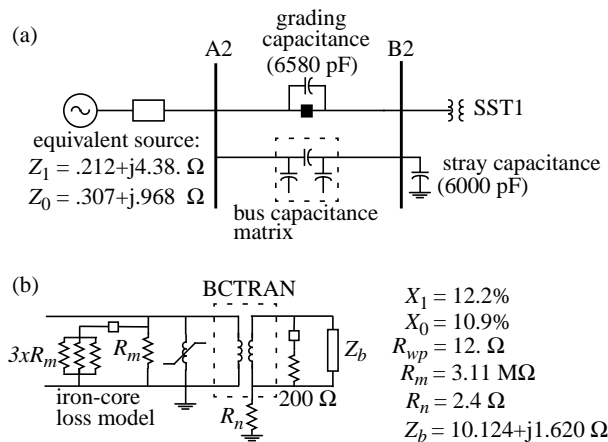


Fig. 2. Single-line diagram of the August 5, 1995, Dorsey disturbance showing (a) main circuit components and (b) model of station service transformer.

The approach taken in modelling the transformer's magnetization curve is to find a polynomial that closely follows the measured data points and best represents recordings from an inrush or ferroresonance test. A 13th order polynomial of the following form is found to be a reasonable representation. Comparison between the two sets are shown in Fig. 3.

$$i(\lambda) = a_1\lambda + a_n\lambda^n \quad (1)$$

Iron-core losses are 17 kW at nominal voltage. A more detailed model of iron-core losses is required to match the recorded transients. The next section discusses iron-core loss modelling in more detail.

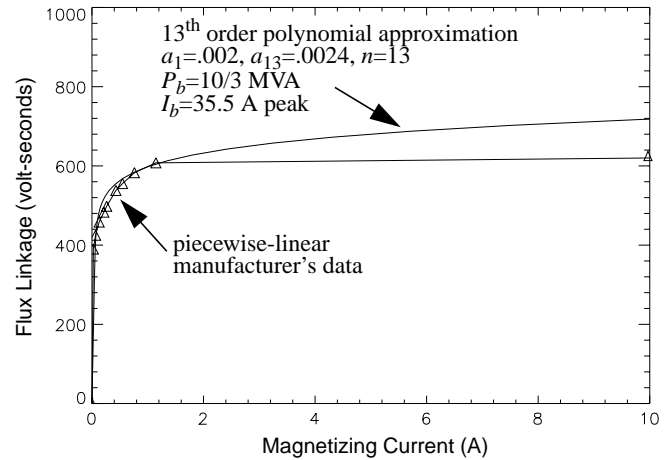


Fig. 3. Station service transformer magnetizing curve.

A. Iron-Core Loss Model

The no-load losses can be categorized into five components: hysteresis losses in the core laminations; eddy-current losses in the core laminations; I^2R losses due to no-load exciting current; stray eddy-current losses in the tank, core clamps, bolts, and other core components; and dielectric losses [3]. Kennedy [3] assumes 99% of the no-load losses are comprised of hysteresis and eddy-current losses. Beckley [4] considers an anomalous loss component arising from the detail of the domain and grain structure of the steel to be significant. Swift defines the anomalous losses as the discrepancy between a classical calculation of eddy-current loss and measurements of the frequency-dependent losses [5]. Janssens *et al.* [6] note that there are supplementary losses occurring in strongly saturated states, such as eddy-current losses in the deflector screens and transformer tank and corona losses.

Historically, the hysteresis losses have been assumed to be 1/3 the eddy current losses for modern transformers constructed using grain-oriented silicon-steel sheets [5]. Janssens *et al.* [6] assumed a 50:50 split between eddy-current and hysteresis losses in their work.

The majority of papers discussing the modelling of losses during ferroresonance have taken Swift's approach and assumed a single linear resistor is adequate to represent all iron-core loss. However, observations made by Walling [7] and Kunde *et al.* [8] indicate that field tests show actual transformers damp transient ferroresonance faster than

calculations predict. Kunde hypothesizes that additional non-measurable losses (i.e. using standard test methods) occur in the transformer.

Janssens *et al.* [6] have used an iterative approach to adapt the value of eddy-current loss and hysteresis loss. An attempt is made to reproduce the correct losses as a function of the amplitude and shape of the oscillation. Measurements of a 245-kV gas-insulated potential transformer show the equivalent iron-core loss conductance can increase to four times its nominal value in strongly saturated states.

Experimental measurements taken on a 2.5-kVA distribution transformer [9] have shown that a three to five-fold decrease in the linear iron-core loss resistor is required to match fundamental frequency losses.

Based on a review of the literature and on experimental tests, it is appropriate to decrease the iron-core loss resistance by a factor of four. At the same instant that the oscillation mode changes to ferroresonance, additional resistance is switched on in parallel with the existing linear iron-core loss resistor. This simple switched resistor model is sufficiently accurate assuming that the oscillation will lock on to the ferroresonant mode.

B. Duplicating Field Measurements

The initial transients of the August 5, 1995 disturbance were not captured. Therefore, details of the fault evolution had to be assumed. A single-phase fault to ground on phase A of the 4.16 kV secondary bus with 0.4 ohm arcing resistance was assumed. The last 230-kV breaker clears 4 cycles after the fault. The 4.16-kV breaker clears the load and fault 7 cycles after the fault. Extra eddy current losses are switched on 8.5 cycles after the fault during the transition to ferroresonance. Fig. 4 details the transient which initiates the ferroresonant oscillations.

Fig. 5 shows the final steady-state ferroresonant mode produced by the EMTF model. The shape and phase of the simulated steady-state oscillations closely match the field recordings given in Fig. 1. However, the magnitudes of the individual harmonic components show some discrepancy, which means a more detailed system equivalent may be necessary to exactly match the ferroresonant oscillation mode.

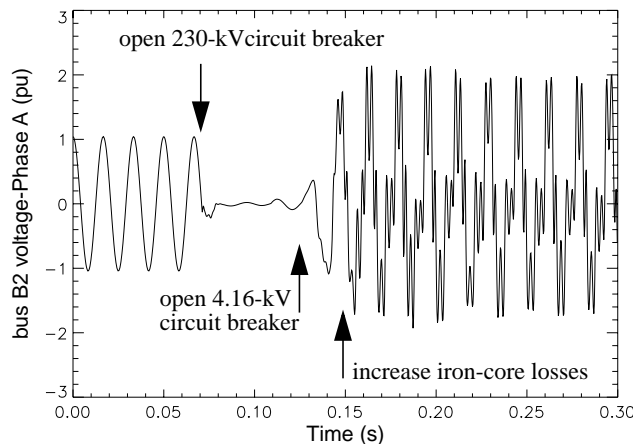


Fig. 4. Initiating ferroresonance in a SST.

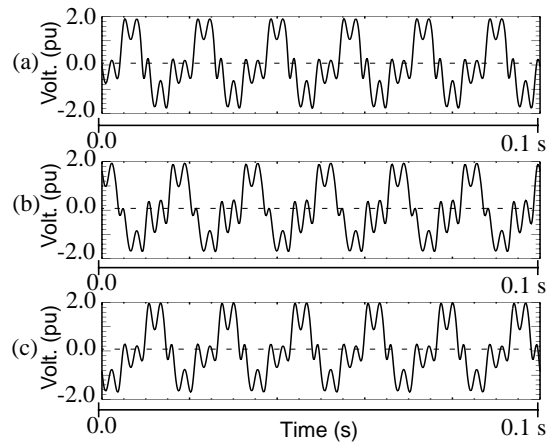


Fig. 5. EMTF simulations showing bus B2 voltage (a) phase C, (b) phase B, (c) phase A.

IV. DESCRIPTION OF DORSEY BUS ENHANCEMENT

A plan is in place to enhance the reliability of the station by adding a third bus and several new bus tie breakers and disconnects. By October 2003, the Dorsey station will be modified as indicated by the single-line diagram given in Fig. 6. The long buses have now been split into three shorter sections. Buses A1 and B1 remain unchanged.

Since the May 20, 1995, destruction of wound potential transformer V13F [1], all wound potential transformers of concern at the Dorsey Station have been replaced with capacitor voltage transformers. Permanently connected 200-Ω loading resistors are installed on the 4.16-kV secondary bus of station service transformers SST1 and SST2 to prevent a recurrence of the August 5, 1995 ferroresonant event.

Because of the bus configuration change, there may be an opportunity for removing the loading resistors if the potential for period-1 ferroresonance is eliminated.

Estimates of the possible combinations of stray and grading capacitance in which the station service transformers may operate are shown in Fig. 7.

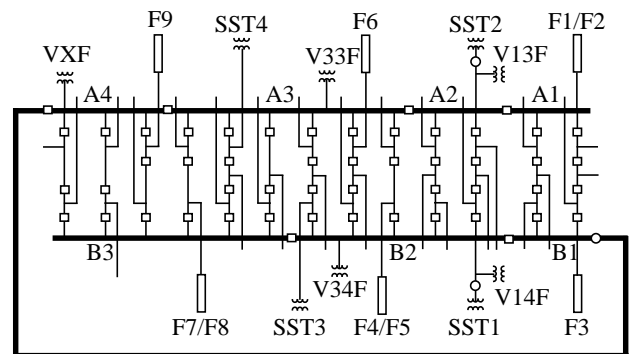


Fig. 6. Dorsey bus enhancement project.

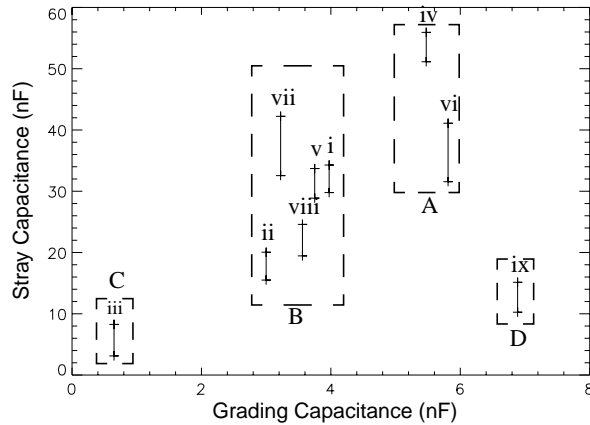


Fig. 7. Dorsey station service transformer stray and grading capacitance operating environment.

The specific configurations correspond to:

- i. normal clearing of SST1
- ii. normal clearing of SST2
- iii. normal clearing of SST3 or SST4
- iv. breaker fail clearing of SST1
- v. breaker fail clearing of SST2
- vi. breaker fail clearing of SST2
- vii. breaker fail clearing of SST3
- viii. breaker fail clearing of SST4
- ix. normal clearing of SST2 (existing configuration)

The configurations have been grouped into four data clusters for later evaluation.

V. FERRORESONANT STABILITY DOMAIN CALCULATIONS

Two different methods of calculating the stability domain boundary between normal 60 Hz oscillations and fundamental frequency (period-1) ferroresonance are compared in this section.

A. Brute Force Method

The brute-force method consists of repeated time-domain simulations followed by frequency-domain analysis of the final steady-state to determine the attractor's periodicity. A consistent set of initial conditions is applied by opening the circuit breaker at the same current zero crossing. The brute-force method is accurate but suffers from a computational disadvantage because several thousand time-domain simulations are required before a sufficiently detailed parameter plane map is produced.

Fig. 8 and Fig. 9 compare the calculated brute-force stability boundaries of faulted and unfaulted clearing of a station service transformer. Faulted clearing is a more severe event that results in a larger portion of the parameter plane having period-1 ferroresonant states. Subharmonic modes do not develop because of the increased stray losses.

A comparison was made between a three-phase transformer model versus three single-phase transformers. It was found that the stability domain boundary was unaffected by the modelling change even though the shapes of the final period-1 attractors were very different.

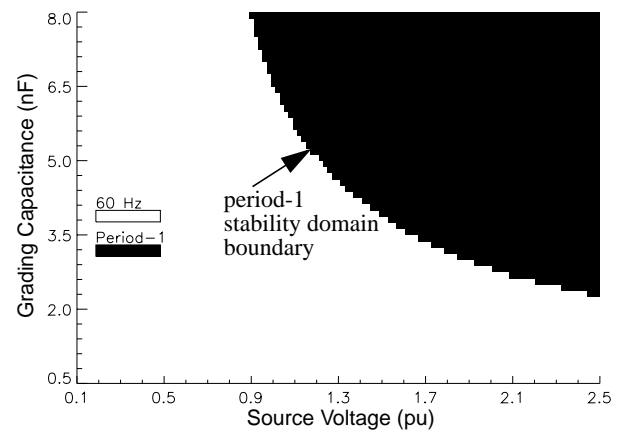


Fig. 8. Faulted clearing of SST1.

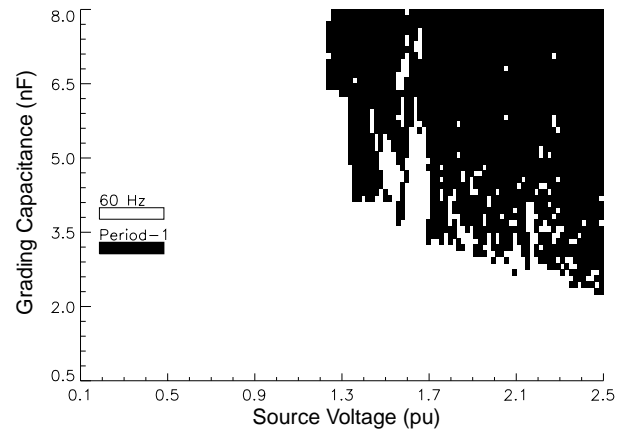


Fig. 9. Unfaulted clearing of SST1.

B. Analytical Method

The curves shown in Fig. 10 are calculated using the equations developed in the Appendix. The essential features of the complete ferroresonant circuit are retained in the simple single-phase circuit, which is used to derive the required equations. First order solutions to the nonlinear differential equation are calculated using the harmonic balance method.

The parameter plane shown in Fig. 10 is divided into several regions depending on the probability of developing ferroresonance. The regions are designated: no risk, low, medium and high risk.

In the low risk region there is a finite probability of developing subharmonic ferroresonance. However, even if a subharmonic state develops, the power losses have been determined to be less than the rating of the transformer.

In the medium risk region, a major disturbance such as fault clearing is required before period-1 ferroresonance occurs. The boundary curve is calculated by projecting the left hand side turning point for the case with four times the normal iron-core losses.

Finally, period-1 ferroresonance develops following normal transformer de-energization in the high risk region. The boundary curve of the high risk region is calculated by determining the parameter values that result in a crossing of the separatrix.

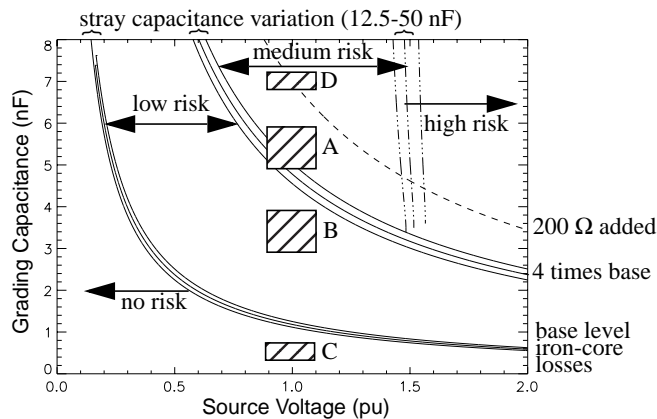


Fig. 10. Display of margin to ferroresonance.

By examining Fig. 10, it is possible to draw the following conclusions:

1. Normal clearing of SST3 or SST4 (Region C) will not result in ferroresonance.

2. Normal clearing of SST1 or SST2 or breaker fail clearing of SST3 or SST4 (Region B) may result in a subharmonic ferroresonance condition. However, the losses associated with such a condition are lower than the transformer's rating and may be tolerated.

3. Breaker fail clearing of SST1 or SST2 (Region A) may result in a period-1 ferroresonance mode similar to the August 5, 1995 disturbance. The probability of faulted clearing with breaker fail is extremely low. Therefore, it is feasible to switch the existing 200 Ω resistors on in this case. The stability domain boundary with the 200 Ω loading resistor added is above Region A, which puts the probability of ferroresonance in the low risk region. Switching of the resistor could be made automatic by modifying the breaker fail protection on two of the new bus tie breakers. Alternatively, the resistors could be closed by an operator.

VI. CONCLUSIONS

Improved analytical techniques show that following completion of the Dorsey bus enhancement project only SST1 and SST2 are at risk of experiencing ferroresonance during a 230-kV breaker fail scenario. Because of the robustness of the station service transformer, it is possible to switch the loading resistors on for this condition only. If the switch fails to close, filter banks can be manually switched onto the bus to remove the ferroresonance situation.

A new method of visualizing the margin between non-ferroresonant and ferroresonant states in a transformer/grading-capacitor circuit has been developed. A general set of averaged equations is derived that permit the analysis of an n^{th} order polynomial approximation of the magnetization curve. The new method will assist utility engineers in quickly assessing the potential risk of ferroresonance in their power system.

VII. REFERENCES

[1] Jacobson, D.A.N., Swatek, D., Mazur, R., "Mitigating Potential Transformer Ferroresonance in a 230 kV Converter Station", *Computer Analysis of Electric Power System*

Transients: Selected Readings, IEEE Press: Piscataway, N.J., pp. 359-365, 1997.

- [2] Jacobson D.A.N., Marti, L., Menzies, R.W., "Modeling Ferroresonance in a 230 kV Transformer-Terminated Double-Circuit Transmission Line", *Proceedings of the 1999 Intl. Conf. on Power Systems Transients*, pp. 451-456, June 20-24, Budapest.
- [3] Kennedy, B.W., *Energy Efficient Transformers*, McGraw-Hill: New York, pp. 30-37, 1998.
- [4] Beckley, P., "Modern Steels for Transformers and Machines", *Power Engineering Journal*, pp. 190-200, August 1999.
- [5] Swift, G.W., "Power Transformer Core Behavior Under Transient Conditions", *IEEE Trans. on Power Apparatus and Systems*, Vol. PAS-90, No. 5, pp. 2206-2210, September/October 1971.
- [6] Janssens, N., Vandestockt, V., Denoel, H., and Monfils, P.A., "Elimination of Temporary Overvoltages Due to Ferroresonance of Voltage Transformers: Design and Testing of a Damping System", *1990 CIGRE*, paper 33-204, pp. 1-8, Sept. 1990.
- [7] Short, T., Burke, J., Mancao, R., "Application of MOVs in the Distribution Environment", *IEEE Trans. on Power Delivery*, Vol. 9 No. 1, pp. 293-305, Jan. 1994.
- [8] Kunde, K., Niedung, L., and Umlauf, A., "Damping Ferroresonance in Transmission Networks", *Power Technology International*, pp. 100-103, Spring 1996.
- [9] Jacobson, D.A.N., *Field Testing, Modelling and Analysis of Ferroresonance in a High Voltage Power System*, Ph.D. Thesis, University of Manitoba, August 2000.
- [10] Jacobson, D.A.N., Lehn, P.W., Menzies, R.W., "Stability Domain Calculations of Period-1 Ferroresonance in a Nonlinear Resonant Circuit", TR10 056 1999, submitted to the IEEE PES for review.

VIII. APPENDIX: EQUATION DEVELOPMENT

Displaying margins to ferroresonance (e.g. Fig. 10) can be achieved rapidly by the straightforward application of a few equations. The method consists of the following basic operations:

1. Calculate all fixed points as a function of the source voltage, while holding other system parameters constant. Determine saddle points by calculating eigenvalues of the Jacobian.

2. Determine turning points or bifurcation points iteratively by combining the harmonic balance equations with the determinant of the Jacobian. The extreme values of the vector of saddle points calculated in the first step is used to initialize the Newton Raphson method.

3. Free a second parameter (i.e. grading capacitance) and project the set of turning points on the grading-capacitance/source-voltage parameter plane.

4. Repeat the above set of calculations at four times the base level of iron-core losses.

5. An improved estimate of the jump to ferroresonance can be calculated by assuming that a double saddle loop (i.e. Limacon of Pascal) can be calculated that is a reasonable estimate of the period-1 separatrix. Once the location of the separatrix is known, the parameter values that result in a crossing from one basin of attraction to another can be calculated.

A. Determining Fixed Points

The magnetizing curve of an actual transformer can be represented by anywhere between a 9th order and a 19th order polynomial approximation. In order to accommodate such a variety of characteristics, a set of averaged equations are derived that allow a general n^{th} order polynomial relation to be used.

Given the simple circuit shown in Fig. 11, which could represent a potential or station service transformer in series with a grading capacitor, a nonlinear differential equation for flux linkage(λ) is desired. The circuit assumes a strong source impedance and transformer with negligible winding resistance.

The differential equation to be solved is given by (2),

$$\ddot{\lambda} + k\dot{\lambda} + C_1\lambda + C_3\lambda^n = G\cos(\omega t), \quad (2)$$

where $k=1/R_m C$, $C_1=\omega_b I_b a_1 / CV_b$, $C_3=\omega_b I_b a_n / CV_b$, and $G=\omega_b \omega V_m / V_b$.

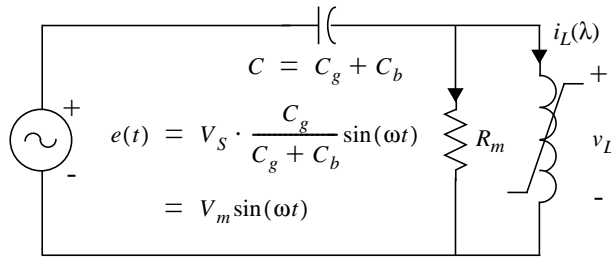


Fig. 11. Simple ferroresonant circuit for developing the equations for the analytical method.

A first-order solution to (2) can be assumed to be of the form:

$$\lambda(t) = a(t)\cos(\omega t) + b(t)\sin(\omega t) = r(t)\cos(\omega t + \theta) \quad (3)$$

The method of harmonic balance requires the assumed solution (3) to be substituted into (2) and the coefficients of sin and cos equated. After equating terms and solving for the first derivative of a and b , the following averaged equations result:

$$\dot{a} = A(a, b) = \frac{-b}{2\omega} \left((\omega^2 - C_1) - C_3(a^2 + b^2)^{\frac{n-1}{2}} d_1 \right) - \frac{ka}{2}, \quad (4)$$

$$\dot{b} = B(a, b) = \frac{a}{2\omega} \left((\omega^2 - C_1) - C_3(a^2 + b^2)^{\frac{n-1}{2}} d_1 \right) - \frac{kb}{2}. \quad (5)$$

By making use of the binomial expansion, d_1 can be written as,

$$d_1 = \left(\frac{1}{2}\right)^{n-1} \binom{n}{(n-1)/2}. \quad (6)$$

Squaring and adding (4) and (5) and substituting $R=a^2+b^2$ results in the following amplitude equation.

$$G^2 = ((\omega^2 - C_1)^2 + k^2\omega^2)R - 2C_3d_1(\omega^2 - C_1)R^{\frac{n+1}{2}} + C_3^2d_1^2 R^n \quad (7)$$

Real values of R that satisfy (7) are substituted into (4)

and (5) in order to determine equilibrium points. Stability of the equilibrium points is determined by calculating the eigenvalues of the Jacobian,

$$\begin{bmatrix} \dot{\xi}_1 \\ \dot{\xi}_2 \end{bmatrix} = \begin{bmatrix} \frac{\partial}{\partial a}A(a_i, b_i) & \frac{\partial}{\partial b}A(a_i, b_i) \\ \frac{\partial}{\partial a}B(a_i, b_i) & \frac{\partial}{\partial b}B(a_i, b_i) \end{bmatrix} \begin{bmatrix} \xi_1 \\ \xi_2 \end{bmatrix}. \quad (8)$$

Given a general n^{th} order polynomial representation of the saturation curve, (4)-(7) and the determinant of the Jacobian can be used to determine the stable fixed points, unstable fixed point and slope through the unstable fixed point as a function of the network parameters.

B. Locating the Separatrix

The separatrix may be computed by time-domain simulation of (4) and (5) for decreasing time if the system states are initialized to the unstable fixed point plus a small deviation along the stable eigenvector associated with this point.

In the conservative case, the general shape of the period-1 separatrix likens that of the geometrical figure known as the Limacon of Pascal [10]. This likeness of the period-1 separatrix to the Limacon of Pascal identifies the following class of functions as candidates for the solution of the separatrix.

$$a(\theta) = \alpha\cos\theta + \beta\cos 2\theta \quad (9)$$

$$b(\theta) = \alpha\sin\theta + \beta\sin 2\theta \quad (10)$$

The exact location of the separatrix for the lossy case can be calculated given the location of the saddle point (a_i, b_i) and the slope of the stable manifold (n_s) through the saddle point. Three equations in three unknowns (α, β, θ) are setup.

$$a_i = \alpha\cos\theta + \beta\cos 2\theta \quad (11)$$

$$b_i = \alpha\sin\theta + \beta\sin 2\theta \quad (12)$$

$$\frac{1}{n_s} = \frac{-\alpha\sin\theta - 2\beta\sin 2\theta}{\alpha\cos\theta + 2\beta\cos 2\theta} \quad (13)$$

After some manipulations, an equation in θ can be derived.

$$0 = \left(\frac{2a_i}{n_s} + b_i\right)\tan\theta^3 - \left(2a_i + \frac{b_i}{n_s}\right)\tan\theta^2 + 3b_i\tan\theta + \frac{b_i}{n_s} \quad (14)$$

After solving for θ , the new Limacon of Pascal constants can be calculated.

$$\beta = -a_i + \frac{b_i}{\tan\theta} \quad (15)$$

$$\alpha = \frac{a_i - \beta\cos 2\theta}{\cos\theta} \quad (16)$$

The lossy Limacon technique determines the parameter values that result in crossing of the separatrix, using only the calculated location of the unstable fixed point and slope through the unstable fixed point.

The parameter value (e.g. V_s) that result in crossing of the separatrix is found iteratively using the simple function $\beta(V_s, C_g) - V_s = 0.0$.